Determination of the longitudinal scattering fraction in $pp \to W^{\pm}W^{\pm}jj$ using a deep machine learning technique

(Dated: July 6, 2015)

The unitarization of the longitudinal vector boson scattering (VBS) cross section by the Higgs boson is a fundamental prediction of the Standard Model which has not been experimentally verified. In the first LHC run, both the ATLAS and CMS collaborations presented first studies of VBS processes in events with two leptonically-decaying same-electric-charge W bosons produced in association with two jets. This channel has the advantage of smaller backgrounds compared to other VBS channels while still exhibiting a detectable production rate. However, the angular distributions of the leptons in the W boson rest frame, which are commonly used to fit polarization fractions, are not readily available in this process due to the presence of two neutrinos in the final state. In this paper we present a method to circumvent this problem by using a deep machine learning technique to recover these angular distributions from measurable event kinematics to determine the longitudinal scattering fraction. We compare the results obtained from this method with other traditional methods. The method presented here can be used as well in other VBS channels with neutrino(s) in the final state.

PACS numbers: 14.70m

I. INTRODUCTION

The discovery of a Higgs-like boson at the LHC [1, 2] was the first step toward a better understanding of the electroweak symmetry breaking (EWSB) mechanism. One important, and unverified, prediction of the Standard Model (SM) is that the scattering amplitude of longitudinal vector bosons ($V_LV_L \to V_LV_L$) is unitarized by the Higgs boson. Measuring VBS processes at a hadron collider, however, is experimentally challenging. Both ATLAS and CMS collaborations recently provided the first evidence of a VBS process using events with two same-sign W boson in association with two forward jets ($pp \to W^{\pm}W^{\pm}jj$) [3, 4]. This final state has the advantage of relatively small SM background contributions compared with other VBS processes. While an ideal candidate for first observing the VBS process, measuring the longitudinal fraction of these events is not straight forward.

In general the polarization of a gauge boson can be determined from the angular distribution of its decay products. Since a W boson only couples to left-handed particles and right-handed anti-particles. In the rest frame of the W boson, the decayed charged lepton is expected to preferentially pointing in the W boson spin direction for W^+ and in the opposite W boson spin direction for W^-. The normalized differential cross section of a leptonically-decaying W boson can be written in terms of polarization fractions as

$$\frac{1}{\sigma}\frac{d\sigma}{d\cos\theta^*} = \frac{3}{8}f_-(1\mp\cos\theta^*)^2 + \frac{3}{8}f_+(1\pm\cos\theta^*)^2 + \frac{3}{4}f_L(1-\cos^2\theta^*), \text{for } W^{\pm} \quad (1)$$

where θ^* is the decay angle defined in the W's rest frame as the angle between the charged lepton and the W boson direction of motion. The three fraction parameters f_-, f_+ and f_L denote the fractions of W events with three possible helicity states -1, $+1$ and 0, respectively. The fs are subjected to the constraint $f_- + f_+ + f_L = 1$. To measure θ^*, we need to fully reconstruct the direction of motion and also the center-of-mass of the W boson.

To determine the charge of each W boson, we require both bosons decay leptonically in the $pp \to W^{\pm}W^{\pm}jj$ events which results in two neutrinos in the final state. Since neutrinos escape the detection, the W boson's rest frames cannot be directly measured. It is thus difficult to determine the polarization fractions of each boson and the fraction of longitudinal scattering events in the $W^{\pm}W^{\pm}jj$ process.

Many proposals have been made to determine longitudinal fractions in other VBS final states, such as semileptonic WW [5], WZ [**?**] and ZZ (le houche report) or fully-leptonic WZ and ZZ, where full event kinematics could be reconstructed. However, these channels either suffer from large SM backgrounds not present in the $W^{\pm}W^{\pm}jj$ channel or have relatively low production cross sections. Attempts have been made to gain sensitivity through other variables than θ^* in the $W^{\pm}W^{\pm}jj$ channel. One example is the variable $R_{p_T} = (p_T^{\ell 1} \times p_T^{\ell 2})/(p_T^{j_1} \times p_T^{j_2})$ shown in [6], where ℓ_1 and ℓ_2 denote the two leptons in no particular order and j_1 and j_2 denote the two most energetic jets in the event. It is natural to assume that all of the sensitivity to longitudinal scattering is not encompassed in a single variable, and that better discrimination could be obtained by combining all the event information with a machine learning technique. In this paper we develope a method to use a neural network to map measurable quantities to the truth $\cos\theta^*$ values that contain the polarization information of the two W bosons.

II. MACHINE LEARNING MODEL

While it has become common practice in high energy physics to use multi-variate techniques to separate signal from background, to the author's knowledge multivariate regression has not been used to directly predict

underlying quantities. Recent success with deep learning in other areas of HEP [8, 8].

For the $W^{\pm}W^{\pm}jj$ events, we use representative measurable quantities such as the transverse momentum (p_T), pseudorapidity (η) and azimuthal angle (θ) of two leptons and two jets, and x and y components of the missing transverse energy ($\not{E}_T^x$ and $\not{E}_T^y$). The overall number of measurable quantities we used is 14. The goal of the multi-variate technique is thus to find the best mapping from these measurable quantities to the two truth values of $\cos\theta^*$ (one for each W boson) present in each event. We choose a multi-layer neural network with a final output layer with linear activation. The neural network was implemented with the Theano software packages [**?**]. Hyperparameters were tuned by hand, but undoubtedly could be improved. The cost function is defined as the mean error squared as listed below

$$\mathcal{C} = \sum_{i=1}^{N}[(\cos\theta^*_{1,i} - N_{1,i})^2 + (\cos\theta^*_{2,i} - N_{2,i})^2]/2N \quad (2)$$

where N is the overall number of events used, $\cos\theta^*_{1/2,i}$ is the truth value of $\cos\theta^*$ for each W boson with random ordering for the i-th event, and $N_{1,2/i}$ is the value of the two neural network outputs. Stochastic gradient descent algorithm [**?**] is used to find all weights and biases in the neural network that minimizes the overall cost function using a training sample.

We generate *** $W^{\pm}W^{\pm}jj$ events using the MADGRAPH event generator [**?**] at a proton-proton center-of-mass energy of 13 TeV. The NN23l01 parton distribution function [**?**] is used as the default. These events are then passed through the detector response simulation of the ATLAS detector implemented in DELPHES [**?**]. Events are split into three categorizes: 1/4 are used in a training sample, 1/4 are used as a validation test against over training, and the remaining 1/2 are used to build templates and do sensitivities studies. A ** layer neural network with ** hidden neurons and a learning rate of ** is used.

III. SIGNAL MODEL

To reduce the contributions from other SM processes, we apply the following generator level cuts on the $W^{\pm}W^{\pm}jj$ sample:

- Parton $p_T > 20$ GeV and $|\eta| < 5$;
- Lepton $p_T > 10$ GeV and $|\eta| < 2.5$;
- $\Delta R_{jj} > 0.4$, $\Delta R_{\ell\ell} > 0.4$ and $\Delta R_{\ell,j} > 0.4$;
- Invariant mass of the two partons $M_{jj} > 150$ GeV.

The resulting cross section at 13 TeV is 8.4 fb^{-1} which is used to normalized the expected number of signal events.

We will first demonstrate the usefulness of deep learning networks with this general sample and then discuss the effects of cuts to reject other backgrounds as well as detector modeling effects.

Polarization fractions are first obtained on the default sample by fitting the two-dimensional distribution of the truth $\cos\theta^*$ variable for each W boson. In order to fit for these polarization fractions templates must be built for "pure" polarization states. These templates are created by reweighting each event based on the truth $\cos\theta^*$ distribution. The weight W_i for the i-th event is given by $W_i = F_i/n_i$, where n_i is used for the normalization and is defined as

$$n_i = [\frac{3}{8}f_-(1\mp\cos\theta_1^*)^2 + \frac{3}{8}f_+(1\pm\cos\theta_1^*)^2 + \frac{3}{4}f_0(1-\cos^2\theta_1^*)] \times [\frac{3}{8}f_-(1\mp\cos\theta_2^*)^2 + \frac{3}{8}f_+(1\pm\cos\theta_2^*)^2 + \frac{3}{4}f_0(1-\cos^2\theta_2^*)]. \quad (3)$$

F_i represents the six possible polarization states for the two W bosons: Left-Left ($--$), Left-Right ($-+$), Right-Right($++$), Left-Longitudinal ($-L$), Right-Longitudinal ($+L$), or Longitudinal-Longitudinal (LL). They are defined as

$$F_i \in \begin{pmatrix} -- = f_-^2(1\mp\cos\theta_1^*)^2(1\mp\cos\theta_2^*)^2, \\ -+ = f_-f_+[(1\mp\cos\theta_1^*)^2(1\pm\cos\theta_2^*)^2 \\ +(1\pm\cos\theta_1^*)^2(1\mp\cos\theta_2^*)^2], \\ ++ = f_+^2(1\pm\cos\theta_1^*)^2(1\pm\cos\theta_2^*)^2, \\ -L = f_-f_L[(1\mp\cos\theta_1^*)^2(1-\cos^2\theta_2^*) \\ +(1-\cos^2\theta_1^*))(1\mp\cos\theta_2^*)^2], \\ +L = f_+f_L[(1\pm\cos\theta_1^*)^2(1-\cos^2\theta_2^*)) \\ +(1-\cos^2\theta_1^*)(1\pm\cos\theta_2^*)^2], \\ LL = f_L^2(1-\cos^2\theta_1^*))(1-\cos^2\theta_2^*) \end{pmatrix}. \quad (4)$$

Since no ordering is applied to the two bosons we require that the individual polarization fractions f_-,f_+,f_L are the same for both W bosons. For reweighting the original sample f_-, f_+, f_L are take as a function of the invariant mass of the diboson system (M_{WW}). Weights are calculated before any additional event level cuts are made, and the resulting templates are remade for each set of cuts explored. To validate the reweighting procedure, we also generate pure polarization state samples using MADSPIN and compare the obtained events kinematics with those obtained from the reweighted sample. Figure 1 shows the calculated $\cos\theta_1^*$ vs $\cos\theta_2^*$ distribution for all six polarization states.

While there are six possible polarization combinations, not all polarization states are as interesting from the the stand point of new physics, and better measurements can be preformed if assumptions are made. We combine events with both W bosons transversly-polarized as TT which is the sum of $--$, $-+$ and $++$ combinations, events with one W boson transversly-polarized and one W boson longitudinally-polarized as TL which is the sum of $-L$ and $+L$ combinations, and events with both W bosons longitudinally-polarized as LL. Figure 2 shows the calculated $\cos\theta_1^*$ vs $\cos\theta_2^*$ distribution for these three polarization states.

Figure 3 shows the normalized R_{p_T} templates for these three polarization states. The differences at large R_{p_T} indicate the sensitivity of this variable to diferent polarization states.

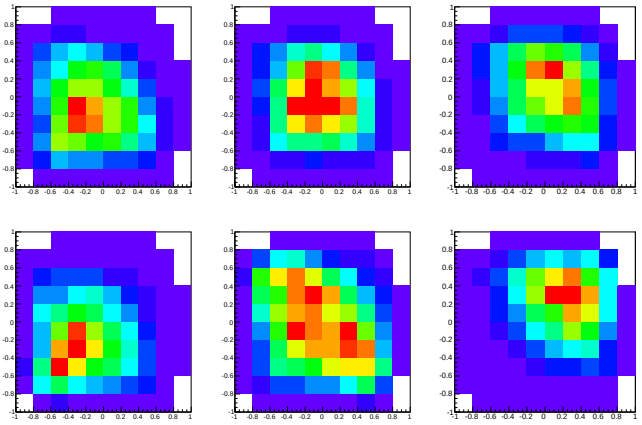

FIG. 1. Two dimensional calculated $\cos\theta_1^*$ vs $\cos\theta_2^*$ templates after reweighting to pure polarization states which clock-wise from the upper left LO,OO,RO,LL,LR,RR.

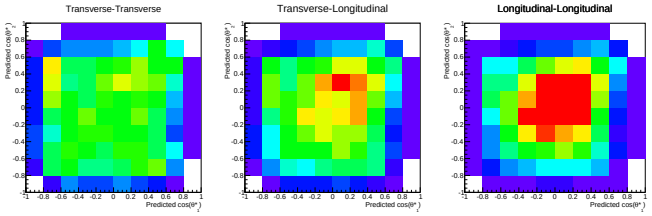

FIG. 2. Two dimensional calculated $\cos\theta_1^*$ vs $\cos\theta_2^*$ templates after reweighting to three polarization states: TT (left), TL (middle) and LL (right).

IV. RESULTS

Armed with templates for each polarization state and a distribution that is sensitive to different polarization states, all we have to do is fit the resulting calculated $\cos\theta_1^*$ vs $\cos\theta_2^*$ two-dimensional distribution in data to derive each polarization fraction. In actual data analysis, this would involve first selecting events to remove SM backgrounds and then subtracting predicted background from data. The effect of additional selection criteria and backgrounds is covered below, but for the case of this section we assume that MADGRAPH selection can be fitted directly to obtain sensitivities. The maximum likelihood fit is preformed with the RooFit framework [**?**]. Fit uncertainties are determined by randomly fluctuating data expectations within their Poisson errors and repeating the fit, and confidence intervals are derived from the toy experiments. To validate the fitting method, we also make sure the fitted values for each fraction agree with with the values obtained at the truth level.

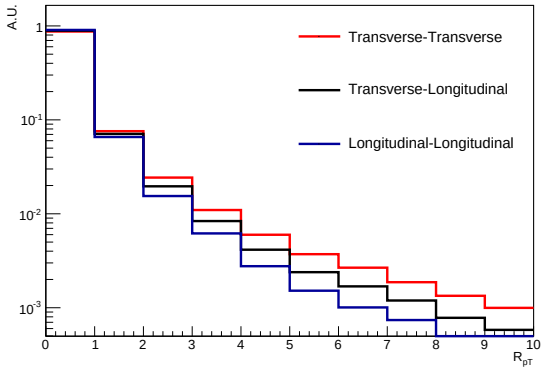

FIG. 3. R_{pT} templates for three polarization states: TT, TL and LL.

The precisions for all six polarization fractions as a function of the integrated luminosity assumed are listed in Fig. 4. The corresponding precisions by fitting the R_{pT} distributions are also shown. Better precisions are obtained for the calculated $\cos\theta^*$ variables which indicate that it is a more sensitive variable to different polarization states than R_{pT}. The precision for the LL fraction is **% (**%) for an integrated luminosity of 100 (3000) fb^{-1}.

The precisions for all three polarization fractions as a function of the integrated luminosity assumed are listed in Fig. 5. The corresponding precisions by fitting the R_{pT} distributions are also shown. It can be seen that as expected better precision can be obtained by reducing the number of templates used. Transverse components can be measured with great precision, whereas separating pure longitudinal-longitudinal scattering from longitudinal-transverse scattering is challenging. However, if we fix the TL fraction to the SM prediction, we can perform a precise measurement of the LL fraction, as shown in Fig. 6. In all cases the neural network output outperforms the R_{pT} variable.

While the success of this neural network at the parton level is encouraging, it is important to check if this procedure will stand up to experimental realities of finite detector resolution and non-VBS background. To reduce SM backgrounds in the loose fiducial region as defined in Sect. III , we apply similar cuts as used by the ATLAS collaboration [3] to obtain a tight fiducial region:

- Jet $p_T > 30$ GeV;
- Lepton $p_T > 25$ GeV;
- $\not{E}_T > 40$ GeV;
- M_{jj} >500 GeV;
- $|\Delta Y_{jj}| > 2.4$.

After the application of these cuts the dominate background comes from the WZ production where one lepton is not detected or not reconstructed. For the generated $W^\pm W^\pm jj$ events, we also use PYTHIA6 for parton shower and hadronization simulation and then pass these events through the DELPHES package (using the CMS simulation card) [**?**] to simulate the detector response of a

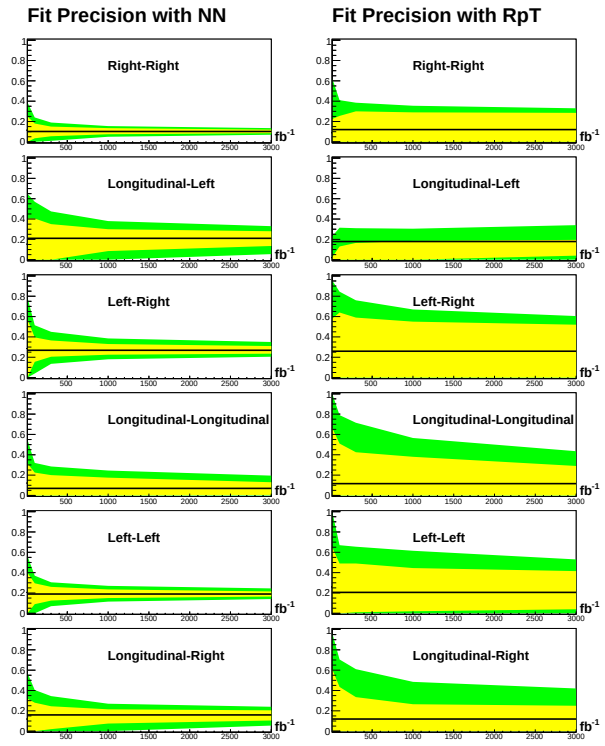

FIG. 4. 68% and 95% confidence intervals for fits with six templates as a function of the integrated luminosity assumed. Fits of the neural network on the left and fits of R_{pT} the on the right.

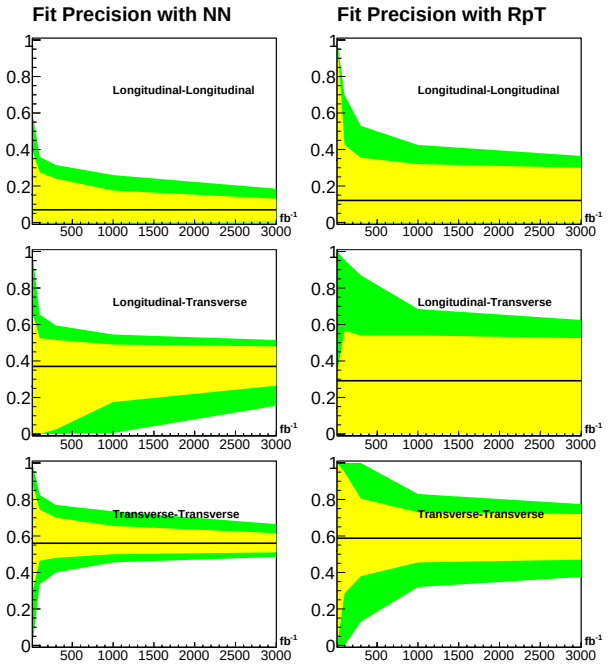

FIG. 5. 68% and 95% confidence intervals for fits with three templates as a function of the integrated luminosity assumed. Fits of the neural network on the left and fits of R_{pT} on the right.

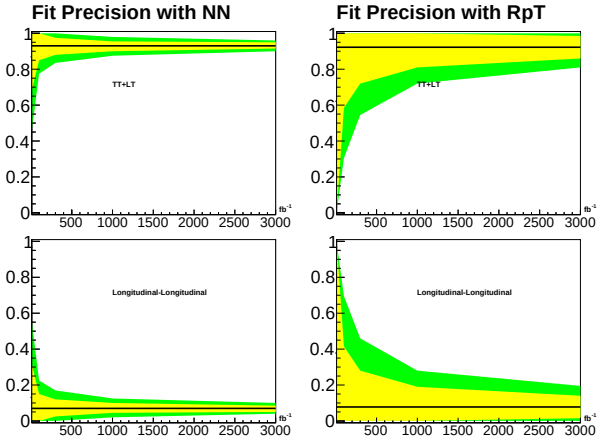

FIG. 6. 68% and 95% confidence intervals for fits with two templates as a function of the integrated luminosity assumed. Fits of the neural network on the left and fits of R_{pT} on the right.

general-purpose particle detector at the LHC. We define the loose and tight fiducial regions at both the parton level and also at the DELPHES level. Table I shows the extracted limits on TT, TL and LL fractions for loose and tight fiducial regions defined at the parton level and at the DELPHES level. Table II shows the corresponding numbers on TT+TL and LL fractions. An integrated luminosity of ** fb^{-1} is assumed.

Figure 7 shows the calculated $\cos\theta^*$ distribution for the dominant WZ background, ++ and LL components of the $W^{\pm}W^{\pm}jj$ events. It can be seen that the calculated $\cos\theta^*$ distribution for the WZ background closely resembles that of the ++ template, it will be important to subtract the WZ contribution before the actual fitting.

Fiducial region	TT		TL		LL	
	LL	UL	LL	UL	LL	UL
Loose (parton level)	0.51	0.62	0.27	0.48	0.01	0.13
Tight (parton level)	0.47	0.63	0.19	0.52	0.0	0.19
Loose (DELPHES level)	0.48	0.65	0.16	0.52	0.0	0.21
Tight (DELPHES level)	0.44	0.66	0.08	0.56	0.0	0.27

TABLE I. Lower Limits (LL) and Upper Limits (UL) on the TT, TL, and LL fractions for loose and tight fiducial regions defined at the parton level and at the DELPHES level.

Fiducial region	TT+TL		LL	
	LL	UL	LL	UL
Loose (parton level)	0.92	0.95	0.05	0.09
Tight (parton level)	0.89	0.95	0.05	0.11
Loose (DELPHES level)	0.9	0.95	0.05	0.11
Tight (DELPHES level)	0.87	0.95	0.05	0.13

TABLE II. Lower Limits (LL) and Upper Limits (UL) on the TT+TL and LL fractions for loose and tight fiducial regions defined at the parton level and at the DELPHES level.

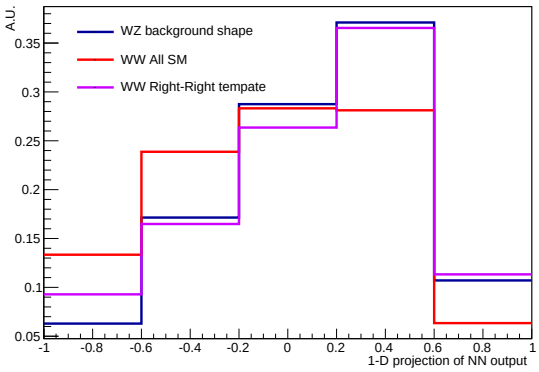

FIG. 7. Signal and background shapes for the calculated $\cos\theta^*$.

V. CONCLUSIONS

We present a method to determine the fraction of each polarization state in the $W^{\pm}W^{\pm}jj$ events by using deep machine learning technique. This method allows us to recover the charged lepton angular distributions from measurable event kinematics. We compare the results obtained from this method and from other traditional methods and show the advantage of our method. Cuts to reject backgrounds as well as detector smearing reduces the sensitivity as expected, but the method remains a useful tool for the study of VBS.

[1] G. Aad *et al.* [ATLAS Collaboration], Phys. Lett. B **716**, 1 (2012) [arXiv:1207.7214 [hep-ex]].

[2] S. Chatrchyan *et al.* [CMS Collaboration], Phys. Lett. B **716**, 30 (2012) [arXiv:1207.7235 [hep-ex]].

[3] G. Aad *et al.* [ATLAS Collaboration], Phys. Rev. Lett. **113**, no. 14, 141803 (2014) [arXiv:1405.6241 [hep-ex]].

[4] V. Khachatryan *et al.* [CMS Collaboration], Phys. Rev. Lett. **114**, no. 5, 051801 (2015) [arXiv:1410.6315 [hep-ex]].

[5] T. Han, D. Krohn, L. T. Wang and W. Zhu, JHEP **1003**, 082 (2010) [arXiv:0911.3656 [hep-ph]].

[6] K. Doroba, J. Kalinowski, J. Kuczmarski, S. Pokorski, J. Rosiek, M. Szleper and S. Tkaczyk, Phys. Rev. D **86**, 036011 (2012) [arXiv:1201.2768 [hep-ph]].

[7] P. Baldi, P. Sadowski and D. Whiteson, Nature Commun. **5**, 4308 (2014) [arXiv:1402.4735 [hep-ph]].

[8] P. Baldi, P. Sadowski and D. Whiteson, Phys. Rev. Lett. **114**, no. 11, 111801 (2015) [arXiv:1410.3469 [hep-ph]].